

Correlation Modeling Between Peening-Induced Hardness, Residual Stress and Roughness in Case-Hardened High Strength Steels

Hsin Shen HO, Cheng LV, Yonghui HE, Erliang ZHANG *

School of Mechanical and Power Engineering and Henan Key Engineering Laboratory of Anti-Fatigue Manufacturing Technology, Zhengzhou University, Science Road 100, 450001, Zhengzhou, China

crossref <http://dx.doi.org/10.5755/j02.ms.24475>

Received 21 October 2019; accepted 22 May 2020

The present paper is focused on the investigation of the correlation modeling of hardness and compressive residual stress on the surface and subsurface regions of case-hardened 18CrNiMo7-6 steels subjected to shot peening. The results exhibit that the relationship between hardness and compressive residual stress can reasonably well be approximated by an inverse linear model. The analysis suggests that the slope and y-intercept of the inverse linear trend line can be related to the compressive residual stress level and the initial material hardness respectively. It is further revealed that the negative effect brought by the peening-induced roughness on the measurement of experimental data computed on the surface can be compensated by performing the normalization using the roughness parameter called the maximum valley height (S_v).

Keywords: high strength steel, shot peening, hardness, residual stress, roughness.

1. INTRODUCTION

Mechanical surface treatments (e.g. shot peening) are widely used in engineering applications to enhance the material properties of mechanical components after thermo-chemical surface treatments (e.g. carburizing). As mechanical treatments are mostly benefitted for producing compressive residual stress, while thermo-chemical treatments are mostly benefitted for increasing hardness, the combination of both is generally applied to create a highly localized plastic deformation for the formation of a deep work-hardened and compressed subsurface layer [1, 2]. Such improved properties can help to increase fatigue strength by retarding fatigue crack initiation on the surface and reducing fatigue crack propagation rate in the subsurface layer [3–6]. As fatigue performance is governed by the combined effects of hardness and compressive residual stress on the surface and subsurface regions [7–10], the assessment of their relations can be useful to determine the expressions that describe their empirical relationships, serving as a tool to predict the properties favourable for enhanced fatigue performance.

In previous study, Llana et al., who focused their investigation on the influence of shot peening intensity on the hardness, compressive residual stress and surface roughness of quenched and tempered AISI 4340 steels, have reported that the (surface and maximum) compressive residual stress and the surface roughness (through R_a and R_{max}) can separately be connected to the hardness through inverse linear relations [8]. But in their studies, the steel initial hardness is used instead of the surface strengthened steel hardness. Though the surface roughness has been recognized as a well-known side effect brought by mechanical treatments, it should however not be disregarded when determining the surface hardness and residual stress because it can cause a serious deviation in the

measurement results [11–13]. Thereby, in another study conducted by Marteau et al., which is focused on the identification of a relation between surface hardening and surface topography induced by shot peening on AISI 316L stainless steels, it has been shown that the best empirical relation between hardness and roughness can well be obtained with the most relevant surface roughness parameter denoted as five point valley height S_{5v} parameter [10].

The present paper aims at investigating the correlations between hardness and compressive residual stress produced by shot peening in case-hardened 18CrNiMo7-6 steels. Furthermore, simple mathematical expressions are provided to evaluate their relations on the surface and subsurface regions. As peening-induced roughness elements are present on the surface, they could be an obstacle to the measurement of experimental data computed on the surface, and thereby, effort is also made to examine how surface topography can be disregarded when assessing the correlation modeling of surface hardness and surface compressive residual stress.

2. EXPERIMENTAL DETAILS

2.1. Material

The target material is a case-hardened 18CrNiMo7-6 steel treated using heat treatment conditions in agreement to ANSI/AGMA B89-2004 [14], with its initial chemical composition of (in wt.%) C: 0.15–0.21, S ≤ 0.035, Si ≤ 0.40, Mn: 0.50–0.90, P ≤ 0.025, Cr: 1.50–1.80, Ni: 1.40–1.70, Mo: 0.25–0.35, Fe: balance.

2.2. Shot peening treatment

Shot peening is performed with the air blast shot peening machine. The specimens are treated by shot peening

* Corresponding author. Tel.: +86-6778 1235.

E-mail address: erliang.zhang@zzu.edu.cn (E. Zhang)

with different intensities and shot diameters. The intensities of shot peening measured by the arc height of Almen specimens are within the range of 0.25 mmA and 0.45 mmA. Cast steel balls with diameters of 0.3 mm and 0.6 mm are selected as shot blasting media. The coverage of 200 % is employed for all peening processes, which is by doubling the exposure time needed to achieve full coverage (100 %). The different shot peening configurations of immediate interest that are applied in the present study are detailed in Table 1.

Table 1. Shot peening parameters of immediate interest.

Variant	Shot diameter, mm	Coverage, %	Almen intensity, mmA
CP0	–	–	–
CP1	0.3	200	0.25
CP2	0.6	200	0.25
CP3	0.6	200	0.45
CP4	0.6 0.3	200	0.45 0.25

2.3. Measurement methods

The hardness is measured along the depth of the cross-section of specimens using a Vickers hardness tester with a load of 200 g and a holding time of 10 s. Considering the material's heterogeneities and measurement errors, three hardness measurements are acquired at each depth, whose average values are used.

The residual stress is measured by the X-ray stress analyzer (LXRD, Proto, Canada) using Cr-K α radiation and the martensitic {211} crystalline plane. The voltage and current are respectively 30 kV and 25 mA. The measured interference peaks are evaluated by the $\sin 2\psi$ method with the diffraction angle (2θ) varying from -45° and 45° . The in-depth profiles of the residual stresses are determined by performing first iterative electrolytic removal of thin surface layers followed by X-ray in-depth measurements.

The surface states of the specimens are examined by Veeco Wyko NPFLEX optical profiler. The measured surface topographies are characterized by five amplitude surface roughness parameters, which are frequently used to measure vertical characteristics of the surface deviation [15]. These parameters, which are computed in agreement to ISO 25178-2012 [16], include arithmetic mean height (S_a), root mean square (S_q), maximum height (S_z), maximum peak height (S_p) and maximum pit height (S_v). Taking into account the spatial surface roughness variations, the presented surface roughness data are the values averaged over three measurement zones on each specimen.

3. RESULTS AND DISCUSSION

3.1. Analyses of (sub)surface layer properties

3.1.1. Surface finish

Fig. 1, presenting the surface topographies of shot peened specimens, shows that shot peening is a process which is capable of producing surfaces with a rather high degree of roughness.

The surface states of all investigated specimens are discussed in the following using the roughness parameter S_a , commonly used for description of an overall measure of the

texture comprising the surface (*cf.* Table 2).

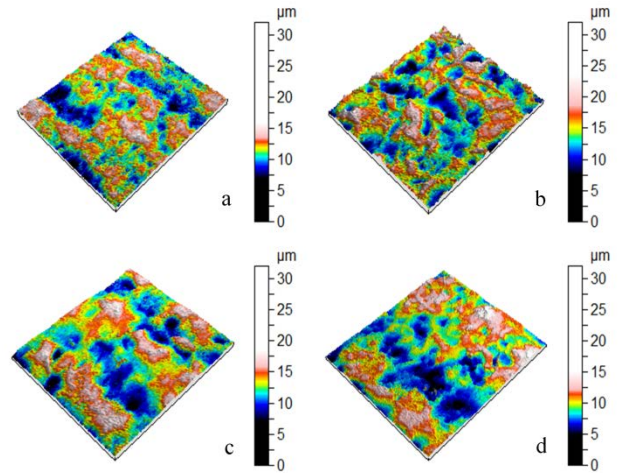


Fig. 1. Surface topographies: a – CP1; b – CP2; c – CP3 and d – CP4 specimens

For CP0 specimen, the S_a value is equal to 2.51 μm . From Table 2, it is shown that when Almen intensity is low, the impact of shot peening using fine shots (CP1 specimen, *cf.* Fig. 1 a) is equivalent to the effect of surface polishing. But if larger-sized particles are used (CP2 specimen, *cf.* Fig. 1 b), the roughness level is increased, implying that higher level of plastic deformation is produced and thus, the surface is roughened.

Table 2. Values of the surface roughness parameters defined by ISO 25178 [16]

Amplitude parameters	CP0	CP1	CP2	CP3	CP4
$S_q, \mu\text{m}$	3.10	2.44	3.42	2.68	2.31
$S_p, \mu\text{m}$	11.10	9.98	15.22	12.30	8.38
$S_v, \mu\text{m}$	9.77	10.32	12.94	12.03	8.24
$S_z, \mu\text{m}$	20.88	20.28	28.20	24.28	16.6
$S_a, \mu\text{m}$	2.51	1.97	2.69	1.89	1.86

Table 2 also shows that as the peening intensity increases (CP3 specimen, *cf.* Fig. 1 c), the S_a value decreases, which is found to be in accordance with Refs. [1, 17, 18]. The use of very high energy larger-sized particles can hardly alter the surface roughness due to the attainment of a critical limit of the plastic deformation. Thus, the continuous impingement of the very high energy larger-sized particles on the specimen surface will subsequently flatten the remained high spot areas and thereby, creating a smoother surface with reduced roughness value.

When re-peening process is performed (CP4 specimen, Fig. 1 d), the S_a value of CP4 specimen is found to be quasi-similar to the one of CP3 specimen. The previously used CP3 peening condition has induced a rather regular surface state by smoothing sharp corners and thus, the application of CP1 re-peening process condition, which is deemed to have surface polishing effects, would have generated a very little beneficial effect on the prior-treated surface state. Though the re-peening process produces a quasi-insignificant roughness improvement effect on the prior-treated specimen, it will be shown in the following that the re-peening process can improve the surface and subsurface

layer qualities of 18CrNiMo7-6 steel in terms of hardness and compressive residual stress.

3.1.2. Hardness

In Fig. 2, the in-depth distributions of hardness are presented for all peened specimens. The figure shows that, regardless of peening conditions, the specimens do have a similar variation tendency of hardness distributions, i.e. first increases sharply and attains a peak value, then decreases progressively with increasing depth and finally reaches a constant value. The trend of the decrement in hardness values is mainly caused by the reduction of not only carbon content but also plastic deformation from the surface all the way down to the core [19].

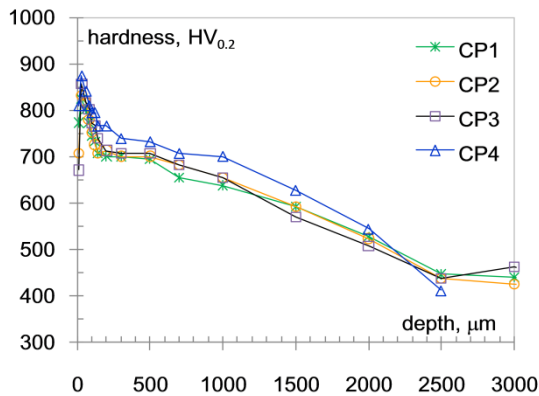


Fig. 2. Hardness distribution curves of all peened specimens

From Fig. 2, it can be seen that the values of surface hardness are much smaller than that of peak hardness, which might be a result of the counteraction of the high surface roughness produced by mechanical surface treatment methods such as machining and shot peening. It can also be observed from the figure that regardless of peening conditions, the case depths are approximated to be $\sim 2450 \mu\text{m}$ while the peening-induced depths are evaluated to be $\sim 120 \mu\text{m}$. In the earlier work, the microstructural alterations such as grain refinement and martensite transformation are very often found to be the principal dislocation-mediated mechanisms by which these highly deformed surface and subsurface regions are formed [4, 19–22].

3.1.3. Residual stress

In Fig. 3, the in-depth distributions of residual stress are depicted for all peened specimens. It can be seen that, regardless of peening conditions, an obvious trend of compressive residual stress distribution is obtained in the surface and subsurface regions; the compressive residual stress first increases to a maximum value, then decreases gradually along the surface layer depth and remains constant thereafter.

Fig. 3 shows that the values of surface compressive residual stress are much smaller than that of peak compressive residual stress. This might be a consequence of the counteraction of initial tensile residual stress and elevated surface roughness developed by the prior surface machining [17]. Regardless of peening conditions, the maximum depths of compressive residual stress are

estimated to be $\sim 90 \mu\text{m}$ while the total depths of compressive residual stress are approximated to be $\sim 300 \mu\text{m}$. This implies that the shot peened specimens have most probably attained the plastic strain limiting values and as a consequence, the continuous impingement of shot particles would not further deepen the depth of the compressed region.

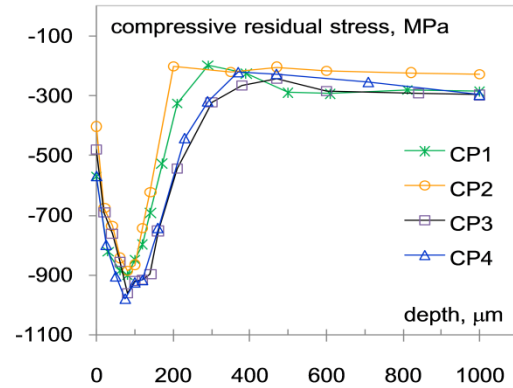


Fig. 3. Compressive residual stress distribution curves of all peened specimens

The above-obtained results show that the effect of shot peening parameters on the incremental of the estimated overall hardness values (*cf.* Fig. 2) can be considered as quasi-trivial as compared with that of the measured overall compressive residual stress values (*cf.* Fig. 3). This observation can mainly be a consequence of:

1. the formation of a very hard case-hardened surface layer by carburizing. Thereby, when shot peening is applied on these very hard carbon-concentrated regions, less localized plastic deformation is produced resulting thus, in an insignificant variation of the overall hardness values regardless of the shot peening conditions;
2. the accommodation of plastic deformation by various dislocation-mediated mechanisms such as generation and rearrangement of dislocations [23]. Thereby, it becomes not unexpected that peening-induced dislocations contribute to plastic strain accumulation which produces high level of compressive residual stress.

The obtained finding suggests that carburizing is more advantageous in terms of hardness distributions while shot peening is more beneficial in terms of compressive residual stress distributions. So, if the combination of carburizing with shot peening is used, a positive synergistic effect can be anticipated, as previously confirmed in Refs. [1, 2].

3.2. Assessment of inter-relationship between hardness-residual stress-roughness

In Fig. 4, the variation of hardness is plotted versus compressive residual stress for carburized specimens subjected to various shot peening treatments. Two distinct correlation regimes can be distinguished: one is for the subsurface (marked by the square symbol in red) and the other one is for the surface (marked by the cross symbol in black). In these two regimes, the hardness (*HV*) is revealed to decrease with the increment of residual stress (*RS*), i.e.

HV is inversely proportional to RS . This suggests the presence of the inverse linear relationship between HV and RS , in coherence with previous work [8]. Giving this proportionality, the relation that relates HV and RS can be expressed as $HV = -a RS + b$, where a and b are the constants that can directly be acquired by the slope and y-intercept of the computed inverse linear regression relationship. The strength of the relationship between HV and RS is then measured using the correlation coefficient value (R^2).

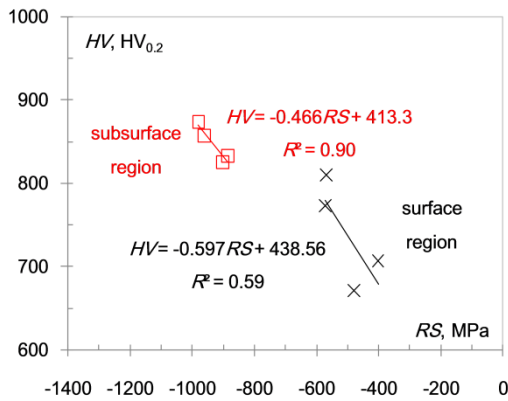


Fig. 4. Modeling of hardness (HV) and residual stress (RS) using linear function

3.2.1. Correlation modeling of hardness and compressive residual stress on the subsurface region

In the first subsurface correlation regime presented in Fig. 4, the functional relationship between peak hardness (HV_{peak}) versus peak residual stress (RS_{peak}) is exhibited. With R^2 -value of 0.90, the supposed inverse linear correlation of HV_{peak} and RS_{peak} can be considered as rather strong and thus, it can be regarded to be rather viable. This finding shows that the contribution of RS_{peak} to HV_{peak} is not negligible, indicating the dependency of HV_{peak} to RS_{peak} .

From Fig. 4, the inverse linear model is found to describe the line between HV_{peak} and RS_{peak} with a value of 0.466 and b value of 413.3. The estimated a -value of 0.466 is found to be quasi-similar to the one obtained in the literature ($a \approx 0.5$) [8], suggesting the efficiency of the inverse linear model in describing the correlation of HV_{peak} and RS_{peak} generated by the combination of shot peening and carburizing. The y-intercept b of 413.3 observed hereby seems to be in contrast with the one obtained in a previously conducted study, showing the absence of the y-intercept in their established mathematical expression that relates RS_{peak} to the initial steel hardness (HV_0). Thereby, the y-intercept b of 413.3 can be considered as the constant concerned with HV_0 , i.e. the hardness of the core material without subjected to any surface treatment method (cf. Fig. 2).

3.2.2. Correlation modeling of hardness and compressive residual stress on the surface region

In the second surface correlation regime, the variation of the surface hardness ($HV_{surface}$) plotted as a function of the surface residual stress ($RS_{surface}$) is given in Fig. 4. From Fig. 4, the inverse linear model, describing the line between $HV_{surface}$ and $RS_{surface}$, yields the a -value of 0.597 and b -value

of 438.56. With this information, two remarks can be made:

1. the a -value (≈ 0.597) calculated in the surface correlation regime, which is noted to be similar to that obtained in the literature (≈ 0.600) [8], is found to be larger than the one computed in the subsurface correlation regime (≈ 0.466). The earlier work shows that the parameter a , which is hereby acquired by the slope of the inverse linear relationships between HV and RS , can be related to the magnitude of compressive residual stress (CRS), which in return can influence the radius size of the contact between indenter and specimen surface that determines HV [24, 25]. Indeed, when the indenter is pressed into the surface with a constant load, CRS tends to push the material towards the indenter surface. This causes the formation of shallower indent with smaller contact radius and as a consequence, the measured hardness value is increased. However, when a very high CRS is present at the surface and subsurface regions, the treated steel is very likely deemed to have attained the critical plastic deformation limit. This would contribute to the decrement of the percentage reduction in indentation depth and size and as a result, the measured difference in hardness is lowered.
2. the b -value (≈ 438.56) computed in the surface correlation regime is observed to be quasi-similar to the one estimated in the subsurface correlation regime (≈ 413.3). This observation once again reaffirms that the parameter b , which is acquired by the y-intercept of the inverse linear relationships between HV and RS , can be the constant corresponded with the initial steel hardness (HV_0).

Though the inverse linear model can adequately be used for description of the correlation between $HV_{surface}$ and $RS_{surface}$, the R^2 -value is however only equal to 0.59, implying that all the experimental surface data are not regression-fitted using the inverse linear method. This is very often stated to be due to roughness elements produced by surface strengthening methods as they could act as local obstructions in the measurement process of experimental data [11 – 13].

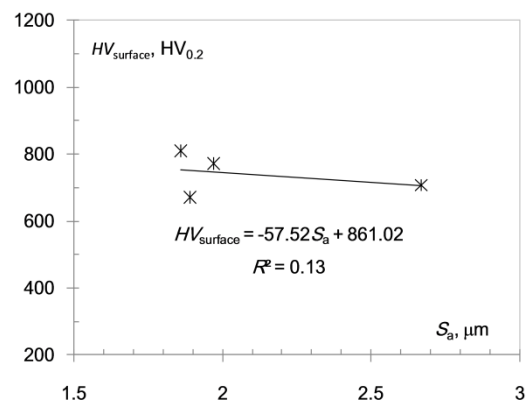


Fig. 5. Variation of surface hardness ($HV_{surface}$) as a function of roughness parameter S_a

In view of the monotonic relationship between $HV_{surface}$ and $RS_{surface}$, the effect of surface roughness will thereby be discussed in the following only with respect to $HV_{surface}$. In Fig. 5, the variation of surface hardness ($HV_{surface}$) with

roughness parameter arithmetic mean deviation (S_a) is presented. It can be seen from Fig. 5 that HV_{surface} is inversely linear proportional to S_a , which is found to be in agreement with results obtained in Ref. [8]. This observation affirms that surface roughness can indeed influence hardness measurement. It is however found that the inverse linear function that relates HV_{surface} to S_a gives an estimated R^2 -value of only 0.13, suggesting that S_a might not be an appropriate parameter for characterizing the peening-induced surface texture as it is unable to fully describe the inherent features of the measured peened surfaces.

In order to find the roughness parameter that can give the best inverse linear relation between HV_{surface} and surface roughness, the correlation coefficient (R^2) is used to measure its strength. In Table 2, all the R^2 values obtained for modeling HV_{surface} and amplitude roughness parameters, e.g. S_q , S_p , S_v , S_z and S_a , are presented. From Table 2, it can be seen that with R^2 value equal to 0.81, the best inverse linear correlation between HV_{surface} and surface roughness is given by the parameter maximum valley height (S_v), defining the area below the average level of a surface. The result is in coherence with that obtained in Ref. [10], where the parameter five point valley heights (S_{5v}) is used to relate hardness of peened specimens with their topography. As parameters S_v and S_{5v} describe the valley heights, they can thereby be considered as directly linked with shot impacts, acting as markers of the plastic deformation. They can thus be used for characterizing shot peened textures and giving a direct linear relationship between valley height and shot penetration.

Table 3. R^2 values estimated from modeling surface hardness and amplitude roughness parameters with linear function

Parameter	S_q	S_p	S_v	S_z	S_a
R^2 value	0.39	0.64	0.81	0.72	0.13

To neglect the negative effect brought by the roughness produced by shot peening, the correlation modeling of HV_{surface} and RS_{surface} is hereby assessed by performing the normalization using the parameter S_v , which is previously identified as relevant in describing the inherent features of shot peened surfaces. In Fig. 6, the variation of HV_{surface}/S_v versus RS_{surface}/S_v is presented.

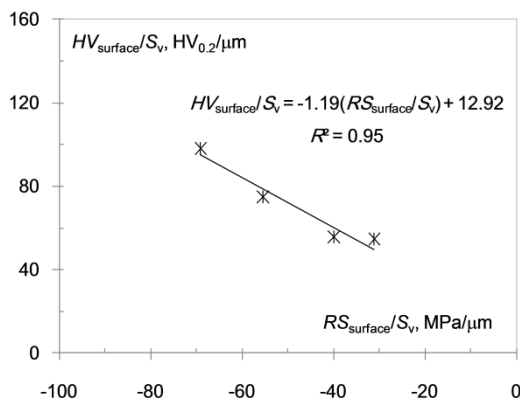


Fig. 6. Modelling of HV_{surface}/S_v and RS_{surface}/S_v with linear function

From Fig. 6, it can be seen that HV_{surface}/S_v is inversely proportional to RS_{surface}/S_v , indicating that the relationship of

HV_{surface}/S_v and RS_{surface}/S_v can reasonably be approximated by an inverse linear model. With the increase of R^2 value from 0.59 (cf. Fig. 4) to 0.95 (cf. Fig. 6), it is hereby suggested that firstly, the contribution of roughness elements to surface measurement data is not ignorable; secondly, S_v is indeed an optimal roughness parameter for characterizing global topography of shot peened surfaces; and thirdly, HV_{surface} and RS_{surface} can well be related to each other when roughness elements are disregarded, as observed in the case of HV_{peak} and RS_{peak} .

4. CONCLUSIONS

In the present work, the relationship between hardness and residual stress is investigated at the surface and subsurface regions of carburized 18CrNiMo7-6 steels after shot peening. The results show that hardness exhibits a monotonically decreasing function with residual stress. It is revealed that the empirical law that relates hardness to residual stress can well be sustained though an inverse linear trend line expressed as $HV = -aRS + b$, with a being the slope of the line and b being the y-intercept. The analyses further suggest that the slope of the line can be related to the magnitude of compressive residual stress while the y-intercept can be connected to the hardness of the core material.

While the peak hardness and peak residual stress exhibit a linear relationship with a correlation coefficient of 0.90, the surface hardness and surface residual stress show a linear relationship with a correlation coefficient of only 0.59. This latter phenomenon occurs mainly due to the presence of peening-induced roughness elements acting as obstructions in measurements of surface hardness and surface residual stress. Thereby, by performing the normalization using a most relevant roughness parameter denoted as maximum valley height (S_v), believed to be capable of fully describing the surface morphology of peened surfaces, the quantitative relationship between surface hardness and surface residual stress are found to be advanced strengthened.

Acknowledgments

This work was supported by the National Natural Science Foundation of China under Grant 51650110502.

REFERENCES

1. **Hassani-Gangaraj, S.M., Moridi, A., Guagliano, M., Ghidini, A., Boniardi, M.** The Effect of Nitriding, Severe Shot Peening and Their Combination on the Fatigue Behavior and Micro-Structure of a Low-Alloy Steel *International Journal of Fatigue* 62 2014: pp. 67–76. <https://doi.org/10.1016/j.ijfatigue.2013.04.017>
2. **Tobola, D., Brostow, W., Czechowski, K., Rusek, P., Wronska, I.** Structure and Properties of Burnished and Nitrided AISI D2 Tool Steel *Materials Science (Medziagotyra)* 21 (4) 2015: pp. 511–516. <http://dx.doi.org/10.5755/j01.ms.21.4.7224>
3. **Hanlon, T., Tabachnikova, E.D., Suresh, S.** Fatigue Behavior of Nanocrystalline Metals and Alloys *International Journal of Fatigue* 27 2005: pp. 1147–1158. <https://doi.org/10.1016/j.ijfatigue.2005.06.035>

4. **Mughrabi, H., Hoppel, H.W., Kautz, M.** Fatigue and Microstructure of Ultrafine-Grained Metals Produced by Severe Plastic Deformation *Scripta Materialia* 51 2004: pp. 807 – 812.
<https://doi.org/10.1016/j.scriptamat.2004.05.012>
5. **Huang, S., Zhu, Y., Gui, W., Peng, P., Qiao, H.C., Diao, X.G., Chu, P.K.** Effects of Laser Shock Processing on Fatigue Crack Growth in Ti-17 Titanium Alloy *Journal of Materials Engineering and Performance* 25 2017: pp. 813 – 821.
<https://doi.org/10.1007/s11665-017-2507-z>
6. **Trsko, L., Guagliano, M., Bokuvka, O., Novy, F., Jambor, M., Florkova, Z.** Influence of Severe Shot Peening on the Surface State and Ultra-High-Cycle Fatigue Behavior of an AW 7075 Aluminum Alloy *Journal of Materials Engineering and Performance* 26 2017: pp. 2784 – 2797.
<https://doi.org/10.1007/s11665-017-2692-9>
7. **Tabor, D.** The Hardness of Materials. Oxford University Press, USA, 1949.
8. **Llaneza, V., Belzunce, F.J.** Study of the Effects Produced by Shot Peening on the Surface of Quenched and Tempered Steels: Roughness, Residual Stresses and Work Hardening *Applied Surface Science* 356 2015: pp. 475 – 485.
<https://doi.org/10.1016/j.apsusc.2015.08.110>
9. **Xie, L., Jiang, C., Lu, W.** The Influence of Shot Peening on the Surface Properties of (TiB + TiC)/Ti-6Al-4V *Applied Surface Science* 280 2013: pp. 981 – 988.
<https://doi.org/10.1016/j.apsusc.2013.05.135>
10. **Marteau, J., Bigerelle, M.** Relation between Surface Hardening and Roughness Induced by Ultrasonic Shot Peening *Tribology International* 83 2015: pp. 105 – 113.
<https://doi.org/10.1016/j.triboint.2014.11.006>
11. **Qasmi, M., Delobelle, P.** Influence of the Average Roughness Rms on the Precision of the Young's Modulus and Hardness Determination Using Nanoindentation Technique with a Berkovich Indenter *Surface and Coating Technology* 201 2006: pp. 1191 – 1199.
<https://doi.org/10.1016/j.surfcoat.2006.01.058>
12. **Bobiji, M.S., Shivakumar, K., Alehossein, H., Venkateshwarlu, V., Biswas, S.K.** Influence of Surface Roughness on the Scatter in Hardness Measurements – a Numerical Study *International Journal of Rock Mechanics and Mining Sciences* 36 1999: pp. 399 – 404.
[https://doi.org/10.1016/S0148-9062\(99\)00009-1](https://doi.org/10.1016/S0148-9062(99)00009-1)
13. **Marteau, J., Bigerelle, M.** Toward an Understanding of the Effect of Surface Roughness on Instrumented Indentation Results *Journal of Materials Science* 52 2017: pp. 7239 – 7255.
<https://doi.org/10.1007/s10853-017-0961-5>
14. **ANSI/AGMA B89.** Gear Material and Heat Treatment Manual American Gear Manufacturers Association. Alexandria, VI, USA, 2004.
15. **ISO 25178-2.** Geometrical Product Specifications (GPS) – Surface Texture: Areal – Part 2: Terms, Definitions and Surface Texture Parameters. 2012.
16. **Gadelmawla, E.S., Koura, M.M., Maksoud, T.M.A., Elewa, I.M., Soliman, H.H.** Roughness Parameters *Journal of Materials Processing Technology* 123 2002: pp. 133 – 145.
[https://doi.org/10.1016/S0924-0136\(02\)00060-2](https://doi.org/10.1016/S0924-0136(02)00060-2)
17. **Lv, Y., Lei, L.Q., Sun, L.N.** Influence of Different Combined Severe Shot Peening and Laser Surface Melting Treatments on the Fatigue Performance of 20CrMnTi Steel Gear *Materials Science and Engineering A* 658 2016: pp. 77 – 85.
<https://doi.org/10.1016/j.msea.2016.01.050>
18. **Unal, O., Varol, R.** Almen Intensity Effect on Microstructure and Mechanical Properties of Low Carbon Steel Subjected to Severe Shot Peening *Applied Surface Science* 290 2014: pp. 40 – 47.
<https://doi.org/10.1016/j.apsusc.2013.10.184>
19. **Li, C.M., He, Q., Tang, W.Z., Lu, F.X.** Carburizing of Steel AISI 1010 by Using a Cathode Arc Plasma Process *Surface and Coating Technology* 187 2004: pp. 1 – 5.
<https://doi.org/10.1016/j.surfcoat.2004.01.026>
20. **Benedetti, M., Fontanari, V., Hohn, B.R., Tobie, T.** Influence of Shot Peening on Bending Tooth Fatigue Limit of Case Hardened Gears *International Journal of Fatigue* 24 2002: pp. 1127 – 1136.
[https://doi.org/10.1016/S0142-1123\(02\)00034-8](https://doi.org/10.1016/S0142-1123(02)00034-8)
21. **An, X.H., Lin, Q.Y., Wu, S.D., Zhang, Z.F.** Improved Fatigue Strengths of Nanocrystalline Cu and Cu-Al Alloys *Materials Research Letters* 3 2015: pp. 135 – 141.
<https://doi.org/10.1080/21663831.2015.1029645>
22. **Tao, N.R., Sui, M.L., Lu, J., Lu, K.** Surface Nanocrystallization of Iron Induced by Ultrasonic Shot Peening *Nanostructured Materials* 11 1999: pp. 433 – 440.
[https://doi.org/10.1016/S0965-9773\(99\)00324-4](https://doi.org/10.1016/S0965-9773(99)00324-4)
23. **Hassani-Gangaraj, S.M., Cho, K.S., Voigt, H.J.L., Guagliano, M., Schuh, C.A.** Experimental Assessment and Simulation of Surface Nanocrystallization by Severe Shot Peening *Acta Materialia* 97 2015: pp. 105 – 115.
<https://doi.org/10.1016/j.actamat.2015.06.054>
24. **Ding, Y., Chromik, R.R.** Relationship Between Indentation Plastic Zone Size and Residual Stresses in Plastically Deformed Fe *Materials Science and Engineering A* 696 2017: pp. 1 – 9.
<https://doi.org/10.1016/j.msea.2017.04.017>
25. **Petrik, J.** The Micro-Hardness of Heat Treated Carbon Steel *Materials science (Medziagotyra)* 20 (1) 2014: pp. 21 – 24.
<http://dx.doi.org/10.5755/j01.ms.20.1.4017>



© Ho et al. 2021 Open Access This article is distributed under the terms of the Creative Commons Attribution 4.0 International License (<http://creativecommons.org/licenses/by/4.0/>), which permits unrestricted use, distribution, and reproduction in any medium, provided you give appropriate credit to the original author(s) and the source, provide a link to the Creative Commons license, and indicate if changes were made.